# Flux reversal time in thin film write heads: A nonlinear system theoretic approach

A. Prabhakar and S. Filips

Citation: Journal of Applied Physics **85**, 6907 (1999); doi: 10.1063/1.370211
View online: http://dx.doi.org/10.1063/1.370211
View Table of Contents: http://scitation.aip.org/content/aip/journal/jap/85/9?ver=pdfcov
Published by the AIP Publishing

# Flux reversal time in thin film write heads: A nonlinear system theoretic approach

A. Prabhakar[a] and S. Filips[b]
*MKE-Quantum Components, 1450 Infinite Drive, Louisville, Colorado 80027*

(Received 28 September 1998; accepted for publication 5 February 1999)

Large amplitude write currents elicit a nonlinear frequency response from thin film write heads. Saturation of the yoke structure causes the measured inductance to be a simultaneous function of both frequency and amplitude. Density plots are used to study the change in inductance over a two dimensional input parameter space comprising ac write current frequency ($1<f<150$ MHz) and dc write current amplitude ($0<I<60$ mA). A simple lumped element reluctance model representing such coupled behavior is proposed. The model extends quasistatic measurements that indicate a quadratic relation between the input magneto-motive force and the magnetic flux in the yoke structure. The circuit consists of a nonlinear reluctance element, described by a Volterra series, connected in series to a linear inductive element. The superposition theorem allows an analytic estimation of the flux reversal time for increasing write current amplitudes. A typical thin film write head that exhibits a quadratic dependence of flux on write current amplitude is analyzed. The model predicts a 30% decrease in flux reversal time over that predicted by a linear model as the amplitude of a stepped input write current is increased by a factor of 10. © *1999 American Institute of Physics.* [S0021-8979(99)09909-0]

## I. INTRODUCTION

The inductive response of a thin film write head is usually measured either as a function of dc write current amplitude at a fixed frequency[1] or as a function of ac write current frequency at a fixed dc write current amplitude.[2] However, saturation of the yoke structure reduces eddy current and domain wall effects causing the inductance to be a simultaneous function of write current amplitude and frequency. It is useful to study changes in the inductance over a two dimensional (2D) input parameter space comprising amplitude and frequency using density plots. Such plots use a color scheme to represent the change in inductance over the amplitude-frequency parameter space. A typical thin film head is studied as we sweep the ac frequency ($1<f<150$ MHz) and gradually step up dc write current amplitude ($0<I<60$ mA). The data clearly show a nonlinear coupling between the yoke inductance and the write current amplitude and frequency.

The Ni–Fe thin film head used in our experiments is typical of those used in current disk drive products. The yoke structure is 20 $\mu$m wide and 35 $\mu$m long, the latter dimension measured as distance from the air bearing surface. The head comprises a single layer 11 turn write coil with a stack height of 12 $\mu$m. These dimensions are approximate and are subject to variations during the manufacturing process. Although the results presented are for measurements on a particular head, the coupled amplitude and frequency dependence of the inductance is observed in a number of samples and is believed to be a characteristic of thin film heads in general. The write coils are often connected to an instrument via a flex interconnect (FIC) that has its own frequency dependent impedance. Using a lossless transmission line model for the FIC, we estimate the maximum frequency to which the observed inductance can be used as a valid measure of the inductance of the yoke structure.

A calculation of the flux reversal time in a thin film write head is complicated by the nonlinear response of the system. Parts of the head get saturated as the write current increases in amplitude. A linear transmission line model can be solved iteratively using a spatially nonuniform permeability distribution to predict the low frequency saturation characteristics of a write head.[3–5] Researchers have also developed a piecewise linear model to study the issue of high frequency write head saturation.[6] However, the use of such iterative procedures on piece-wise linear models does not permit an analytic solution to an inherently nonlinear problem. Furthermore, an input pulse has multiple frequency components. Using a single inductance-saturation curve, measured at a fixed ac write current frequency, to predict the response of the write head can only act as a good first approximation.[7] Our experiments indicate that the inductance-saturation characteristics depend on the frequency of the superimposed ac write current. Hence, it is necessary to develop a model that couples the frequency and saturation response of the write head.

The time domain response of the nonlinear system cannot be related to its frequency response using linear Fourier transforms. There does exist an analytic theory that links time and frequency domain measurements for a nonlinear system[8] where the response of a nonlinear circuit element is represented by a Volterra series. We have developed an analogous nonlinear reluctance model to estimate the dependence of flux reversal time on write current amplitudes as the

[a]Currently at ReadRite Corp., Milpitas, CA 95035.
Electronic mail: anilpr@yahoo.com
[b]Currently at Seagate Storage Products, Longmont, CO 80503.

 

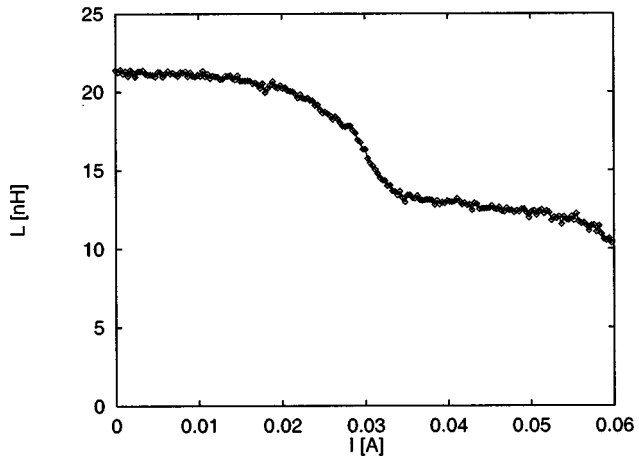


FIG. 1. Write current dependence of the yoke inductance. Yoke inductance is measured as the difference between the unsaturated and saturated write head inductance. The frequency of the small amplitude ac signal was 2 MHz.

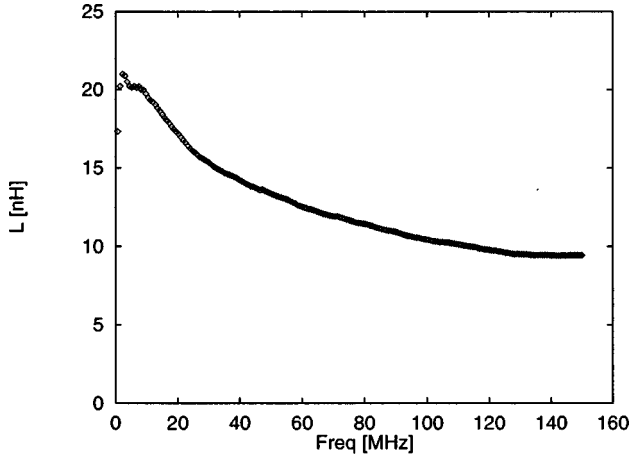


FIG. 2. Frequency dependence of the yoke inductance at zero dc write current. Yoke inductance is measured as the difference between the unsaturated and unsaturated write head inductance. The asymptotic value of $L$ represents the inductance of the air coil with the yoke completely saturated.

write head undergoes saturation. High amplitude pulsed experiments and frequency response experiments are often conducted on thin film heads and their related magnetic materials.[9,10] We hope that the development of a nonlinear system theory will enable researchers to link the time and frequency domain measurements on thin film write heads.

## II. INDUCTANCE MEASUREMENTS

We measure the inductance of a thin film head by superimposing a small amplitude ac signal on a dc write current. The inductance as a function of dc write current provides us with the saturation characteristics of the thin film head. The characteristics are used to understand the response of the head as the yoke structure undergoes spatially nonuniform saturation.[1] The characteristics also form the basis of the saturation sub model used to predict the nonlinear time domain response of the write head.[7] Figure 1 shows the inductance-saturation response of a typical thin film write head with a saturation point at approximately 30 mA. The effects of the FIC between the network analyzer and the yoke structure were minimized by taking the difference between the unsaturated and saturated yoke inductance. Saturation of the yoke structure was achieved by placing the head in an external magnetic field of 2.8 kOe.

When measured as a function of ac signal frequency at a fixed dc write current, the inductance of a thin film head rolls off at high frequencies[2] as shown in Fig. 2. The presence of a FIC limits the maximum frequency to which we can reliably claim to be measuring the inductance of the write head. Assuming that the FIC behaves as a lossless transmission line with characteristic impedance $Z_0$ and resonance radial frequency $\omega_0$, the measured impedance

$$\frac{Z}{Z_0}=\frac{Z_L\cos\theta+jZ_0\sin\theta}{Z_0\cos\theta+jZ_0\sin\theta}, \tag{1}$$

where $\theta=\omega/\omega_0$, $\omega$ is the operating radial frequency and $Z_L$ is the load impedance seen by the FIC. For $\theta^2/2\ll 1$, $\cos\theta \approx 1$ and $\sin\theta\approx\theta$, let us rewrite Eq. (1) as

$$\frac{Z}{Z_0}\approx\frac{Z_L+jZ_0\theta}{Z_0+jZ_L\theta}. \tag{2}$$

The assumption that $\omega\ll\sqrt{2}\omega_0$ allows us to approximate the measured inductance as

$$\frac{1}{\omega}\mathrm{Im}[Z]\triangleq L(\omega)\approx L_{\mathrm{yoke}}(\omega)+L_{\mathrm{flex}}, \tag{3}$$

where $L_{\mathrm{flex}}$ represents the inductive response of the FIC. Typical values for the inductance and capacitance of the FIC are 30 nH and 3 pF, respectively,[11] yielding $Z_0=100\ \Omega$ and $\omega_0=2\pi(530\,\mathrm{MHz})$. Hence, it is reasonable to assume that Eq. (3) is valid to about 150 MHz, where one observes a flattening out of the measured inductance. For higher values of $\omega$, the additive approximation in Eq. (3) breaks down. As $\omega\rightarrow\omega_0$ the frequency response is dominated by that of the FIC and has a resonant effect on the measured impedance.

Figures 1 and 2 establish that the inductance of a write head depends on both the frequency and the saturation characteristics of the yoke structure. Density plots show the changes in inductance as both ac frequency and dc write current amplitude are varied. Figure 3 is a density plot of the unsaturated yoke inductance. A roll-off in inductance occurs as either frequency or current amplitude increase. A similar measurement of the saturated yoke inductance was also taken. Extending the method suggested in Ref. 7, the quasistatic flux is obtained as

$$\Phi(I,\omega)=\frac{1}{N}\int_0^I[L(i,\omega)-L_{\mathrm{sat}}(i,\omega)]di, \tag{4}$$

where $L_{\mathrm{sat}}$ is the saturated yoke inductance. Numerical integration of the inductance data was performed using the trapezoidal rule. A density plot of $\Phi(I,\omega)$ is shown in Fig. 4. Since we are treating $\omega$ as a constant in Eq. (4), the variation in $\Phi$ with increasing frequency follows the frequency dependence of the inductance. We shall attempt to quantify the effects of such a frequency dependence in Sec. III.

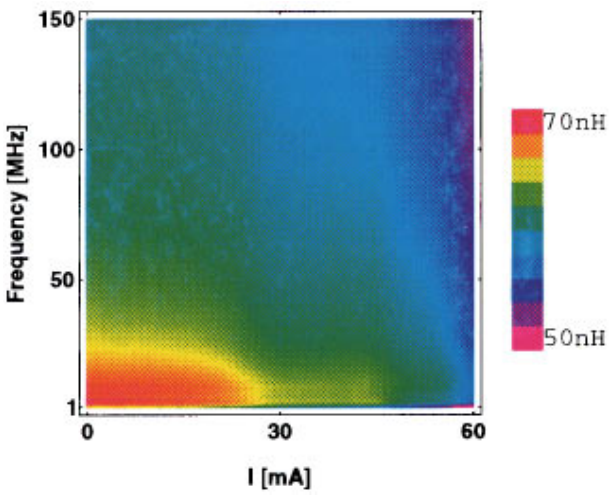


FIG. 3. Variation in unsaturated yoke inductance as a function of input dc write current amplitude and ac write current frequency.

## III. NONLINEAR RELUCTANCE MODEL

Calculations of the deep gap field often rely on a transmission line/head reluctance model.[3,12,13] We use the simple lumped element model shown in Fig. 5 to describe the nonlinear characteristics of the head and choose not to plunge into the complexity of spatially inhomogeneous head saturation. The input voltage, $v(t)$, is equal to the magneto-motive force (MMF) while the current, $i(t)$, represents the magnetic flux in the head, $\phi$. The deep gap flux, $i_g(t)$, is proportional to the MMF, $v_R(t)$, that appears across the combined linear reluctance of the yoke and the air gap, $R$. Since the reluctance of the air gap is much larger than that of the yoke, it is reasonable to assume that $R$ represents the linear reluctance of the air gap. The admittance, $Y_R$, acts as a nonlinear voltage controlled current element and is represented by a linear part in parallel with a current source.

The linear $R$-$L$ circuit acts as a low pass filter with an exponential response and a time constant $\tau = b_1/a_1$. The

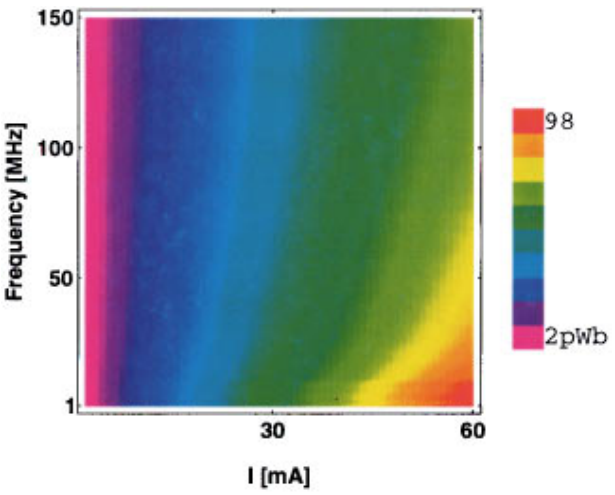


FIG. 4. Variation in yoke flux, as defined by Eq. (4), with changing input dc write current amplitude and ac write current frequency. The data were collected by sweeping frequency in steps of 0.75 MHz and then stepping up dc write current in steps of 1 mA.

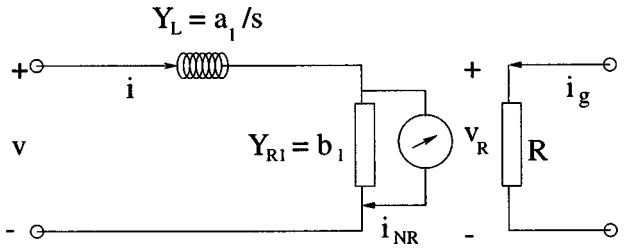


FIG. 5. Nonlinear lumped element circuit for a thin film write head. The input $v(t) \equiv$ MMF, the current $i(t) \equiv \phi$, and the deep gap flux $i_g(t) \propto v_R(t)$.

term $b_1$ is the linear admittance of the resistor and $Y_L = a_1/s$ that of the inductor measured at frequency $s = j\omega$. We choose a circuit with a frequency response that is consistent with the observed decrease in inductance at high frequencies. This simple approximation decouples the frequency response from the saturation effects using a minimum number of circuit elements. However, the circuit introduces a phase lag between the MMF and the flux, reminiscent of the phase lag observed by some researchers.[14] The introduction of any loss mechanism via a complex permeability into a reluctance model will cause such a phase lag. A more accurate match to the frequency response would necessitate the use of a more complicated eddy current model.[7]

Let the time domain characteristics of the nonlinear resistor be expressed as a Volterra series

$$i_R(t) = \sum_{n=1}^{\infty} b_n v_R^n(t) \tag{5}$$

such that the Laplace transform of its admittance is

$$Y_{\mathrm{Rn}}(s_1, s_2, \ldots, s_n) \triangleq b_n \quad \forall n \geqslant 1. \tag{6}$$

The term $i_{\mathrm{NR}}(t)$ represents the nonlinear component of the current through the resistor and is defined as

$$i_{\mathrm{NR}}(t) = i_R(t) - b_1 v_R(t). \tag{7}$$

The coefficients $b_n$ are obtained by fitting the steady state response of the system, $i\ v/s\ v$, to a polynomial. The total flux, $i$, can be obtained by integrating the experimentally measured low frequency $(s \to 0)$ inductance characteristics of the head as a function of bias current.[1] A least squares fit to the experimental data in Fig. 6 indicates that the flux in the head (in pico Webers) can be related to the input MMF (in Ampere turns) via the quadratic equation

$$i_R = 209.4 v_R - 74.3 v_R^2 \quad [R^2 = 0.99]. \tag{8}$$

Despite the good fit to $\phi$, the above equation ignores abrupt saturation effects at 30 mA as seen in Fig. 1. A quadratic model can only account for the gradual linear decrease in inductance with increasing input MMF. An analytic solution to the nonlinear system, as described in Sec. IV, becomes more complicated as we include higher order nonlinear terms.

## IV. ESTIMATING FLUX REVERSAL TIME

The dependence of flux reversal time on current amplitudes is calculated using the superposition theorem. The lin-

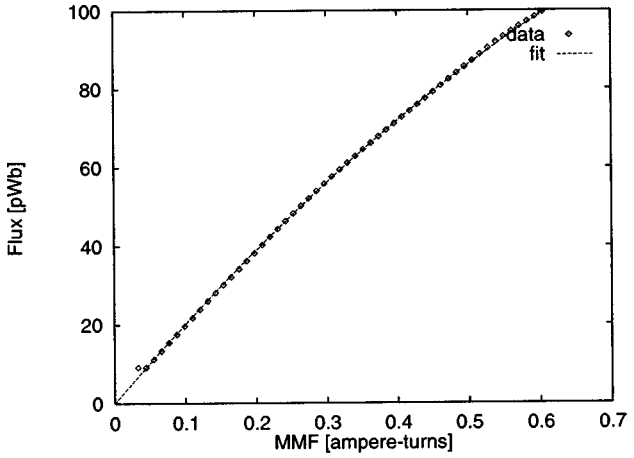


FIG. 6. Change in flux enclosed by the write coils as a function of input MMF, calculated by applying Eq. (4) to the data in Fig. 1. The dashed line is a least squares quadratic fit through the data points, corresponding to Eq. (8).

ear circuit is solved for the potential $V_{R1}$ across the nonlinear element with the current source initially open circuited. We use the value of $V_{R1}$ to determine the value of the nonlinear current source $I_{\mathrm{NR}}$, short the voltage source and then calculate the potential, $V_{R2}$ across the nonlinear element. The total MMF that appears across the linear reluctance $R$, will be the sum of the two potentials. Since $I_{\mathrm{NR}}$ is actually a dependent current source, superposition introduces an error in our analysis. However, with a weak nonlinearity in the system, we expect the error to be small. This approach, as outlined by Chua and Ng,[15] allows us to estimate the nonlinear response of the circuit via Laplace transforms.

An analysis of the circuit in Fig. 5 yields

$$V(s)=I(s)\left[\frac{s}{a_1}+\frac{1}{b_1}\right]-\frac{1}{b_1}I_{\mathrm{NR}}(s), \tag{9}$$

$$V_R(s)=\frac{1}{b_1}[I(s)-I_{\mathrm{NR}}(s)], \tag{10}$$

which can be rewritten as

$$V_R(s)=\frac{1}{\Delta(s)}[a_1-s]\begin{bmatrix}V(s)\\ I_{\mathrm{NR}}(s)\end{bmatrix}, \tag{11}$$

where $\Delta(s)\triangleq a_1+b_1 s=a_1(1+\tau s)$. Setting $I_{\mathrm{NR}}=0$ yields the linear response of the circuit

$$V_{R1}(s)=\frac{a_1}{\Delta(s)}V(s). \tag{12}$$

The nonlinear current is obtained from Eqs. (6) and (12) as

$$I_{\mathrm{NR2}}(s_1,s_2)=Y_{R2}(s_1,s_2)V_{R1}(s_1)V_{R1}(s_2)$$
$$=\frac{b_2 a_1^2}{\Delta(s_1)\Delta(s_2)}V(s_1)V(s_2). \tag{13}$$

With $V(s)=0$ and $s=s_1+s_2$, we obtain the quadratic response from Eq. (11) as

$$V_{R2}(s_1,s_2)=\frac{-(s_1+s_2)}{\Delta(s_1+s_2)}I_{\mathrm{NR2}}(s_1,s_2). \tag{14}$$

To calculate $v_R(t)$, we input a step function of amplitude $V_0$ with a Laplace transform

$$V(s)=\mathcal{L}[v(t)]=\frac{V_0}{s},\quad s>0. \tag{15}$$

Substituting Eq. (15) in Eqs. (12) and (14) yields

$$\frac{V_{R1}(s)}{V_0}=\frac{a_1}{s\Delta(s)}=\frac{1}{s}-\frac{\tau}{1+\tau s}, \tag{16}$$

$$\frac{V_{R2}(s_1,s_2)}{V_0^2}=\frac{(s_1+s_2)a_1^2 b_2}{s_1 s_2\Delta(s_1)\Delta(s_2)\Delta(s_1+s_2)}. \tag{17}$$

$V_{R2}(s_1,s_2)$ is converted back to the form $V_{R2}(s)$ via an *associated transform*[16]

$$V_{R2}(s)=\frac{1}{2\pi i}\int_{\sigma-i\infty}^{\sigma+i\infty}V_{R2}(s-s_2,s_2)e^{s_2 t}ds_2$$
$$=\frac{4V_0^2 b_2}{a_1}\left[\frac{1}{1+\tau s}-\frac{1}{2+\tau s}+\frac{1}{(1+\tau s)^2}\right]. \tag{18}$$

Finally, the time domain response is obtained as

$$v_R(t)=\mathcal{L}^{-1}[V_{R1}(s)+V_{R2}(s)]$$
$$=V_0(1-e^{-t/\tau})+\frac{4V_0^2 b_2}{b_1}e^{-t/\tau}\left(1-\frac{t}{\tau}-e^{-t/\tau}\right). \tag{19}$$

With the deep gap flux $i_g(t)=v_R(t)/R$, its time domain response in terms of a reduced time $t'=t/\tau$ and a nonlinear amplitude $\alpha\triangleq 4V_0 b_2/b_1$, is given by

$$i_g(t')=\frac{V_0}{R}[1-e^{-t'}(1-\alpha+\alpha t')-\alpha e^{-2t'}]. \tag{20}$$

As is expected for a quadratic $R$-$L$ circuit, the time domain response to a step input signal has two decaying exponentials. The quadratic fit to the experimental data, as defined by Eq. (8), yields $4b_2/b_1\approx -1.4[\text{ampere turns}]^{-1}$. The flux reversal time (10%–90% of maximum flux) for the nonlinear circuit is calculated using Eq. (20) and plotted versus write current in Fig. 7.

## V. DISCUSSION

We present experimental evidence that suggests a coupling between the frequency response and the saturation of the yoke structure. The coupling is attributed to nonlinear loss mechanisms such as a dampening of eddy currents with the onset of saturation. Density plots over a two dimensional parameter space comprising of write current amplitude and frequency show a decrease in inductance as either parameter increases. We extend the phenomenological quasistatic determination of yoke flux[7] to include the frequency variations of the yoke inductance. The resulting frequency dependence of the flux is modeled using a nonlinear $R$-$L$ reluctance circuit.

A nonlinear system theoretic approach provides an analytic alternative to contemporary piece-wise linear models used to estimate flux reversal times. Use of the superposition theorem in conjunction with Laplace transforms allows us to

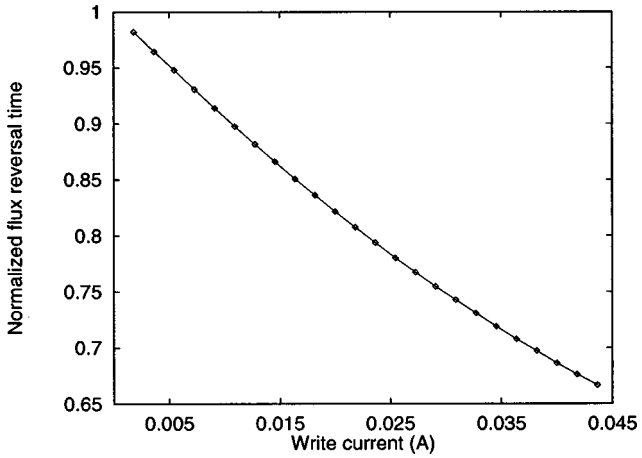


FIG. 7. Amplitude dependence of flux reversal time (10%–90% of maximum flux). The calculation is for reduced time, $t' = t/\tau$, and assumes a step input write current.

predict the time domain response of the yoke flux to a step input write current. For a quadratic system the time domain response of the $R$-$L$ circuit to a step input signal is the sum of two decaying exponentials. We expect that with three filtering segments to model loss mechanism,[7] we would observe a time domain response with up to six decaying exponentials. The present model supports earlier predictions of a decrease in flux reversal time with an increase in write current amplitude.[6,17]

The use of a nonlinear systems approach will enable comparisons between experimental measurements of the pulsed and monotonic frequency response of severely damped magnetic systems.[9,10] It is unfortunate that a direct experimental validation of the theoretical predictions remains difficult. An interpretation of the magneto-optic measurements of the flux reversal time at the pole tips is often complicated by a spatially nonuniform response.[18] The lumped element approach ignores all spatial nonuniformities and can only provide an estimate of the nonlinear time domain response.

[1] A. Payne, P. Thayamballi, and P. Macias, IEEE Trans. Magn. **33**, 2860 (1997).
[2] A. Payne, W. Cain, R. Hempstead, and G. McCrea, IEEE Trans. Magn. **32**, 3518 (1996).
[3] T. C. Arnoldussen, IEEE Trans. Magn. **24**, 2482 (1988).
[4] A. F. Torabi, M. L. Mallary, R. Perry, and G. Kimball, IEEE Trans. Magn. **34**, 1465 (1998).
[5] A. Prabhakar, M. Jursich, K. Wiesen, R. Lansky, and G. Noyes, paper B2 in Digests of The Magnetic Recording Conference (TMRC), Boulder, 1998.
[6] K. B. Klaassen and R. G. Hirko, IEEE Trans. Magn. **32**, 90 (1996).
[7] K. B. Klaassen and R. G. Hirko, IEEE Trans. Magn. **32**, 3524 (1996).
[8] L. Chua and C. Ng, IEE.-G: Electron Circuits Syst. **3**, 165 (1979).
[9] T. Silva, T. M. Crawford, and C. T. Rogers, Paper CA-02 presented at the 7th Joint MMM Intermag Conf., San Francisco, 1998 (unpublished).
[10] B. Argyle, Paper HB-10 in Ref. 9 (unpublished).
[11] A. Balakrishnan and C. M. Carpenter, IEEE Trans. Magn. **34**, 24 (1998).
[12] R. E. Jones, IEEE Trans. Magn. **14**, 509 (1978).
[13] E. P. Valstyn and H. Huang, IEEE Trans. Magn. **29**, 3870 (1993).
[14] N. H. Yeh and K. N. Yang, IEEE Trans. Magn. **29**, 3864 (1993).
[15] L. Chua and C. Ng, IEE.-G: Electron Circuits Syst. **3**, 257 (1979).
[16] W. J. Rugh, *Nonlinear System Theory* (Johns Hopkins University Press, Baltimore, 1981), p. 67.
[17] R. Wood, M. Williams, and J. Hong, IEEE Trans. Magn. **26**, 3954 (1990).
[18] M. R. Freeman, A. Y. Elezzabi, and J. A. H. Stotz, J. Appl. Phys. **81**, 4516 (1997).